Extending the bandwidth of optical-tweezers interferometry

Peterman, E.J.G.; van Dijk, M.A.; Kapitein, L.C.; Schmidt, C.

published in
Review of Scientific Instruments
2003

DOI (link to publisher)
10.1063/1.1584085

document version
Publisher's PDF, also known as Version of record

Extending the bandwidth of optical-tweezers interferometry

Erwin J. G. Peterman,[a] Meindert A. van Dijk, Lukas C. Kapitein, and Christoph F. Schmidt
Department of Physics and Astronomy, Faculty of Sciences, Vrije Universiteit, De Boelelaan 1081, 1081 HV, Amsterdam, The Netherlands

(Received 3 February 2003; accepted 25 April 2003)

High-resolution force and displacement measurements by laser interferometry, combined with optical tweezers in a light microscope, are frequently based on near-infrared lasers. With common silicon PN photodiodes the bandwidth of detection was found to be limited to about 5 kHz at 1064 nm laser wavelength. This is caused by the fact that silicon becomes increasingly transparent for wavelengths approaching the band gap energy, leading to the generation of charge carriers outside the depletion zone of the diode for wavelengths longer than about 850 nm. These charges have to diffuse before they can contribute to the photocurrent. In this technical note we demonstrate experimentally that the detection bandwidth can be extended to at least 100 kHz, either by using wavelengths below 850 nm, or by using different detectors at longer wavelengths: InGaAs PIN photodiodes or special-purpose fully depleted *p*-type silicon photodiodes. We measured the well-known power spectral density of the Brownian motion of micron-sized beads in optical tweezers and show that the optimized detectors do not cause attenuation within experimental noise. They are indeed linear enough to detect the weak inertial effects of the watery solvent on the power spectral density of the Brownian motion. © *2003 American Institute of Physics.*
[DOI: 10.1063/1.1584085]

I. INTRODUCTION

Optical tweezers are a versatile tool to manipulate micrometer-sized objects and to measure forces in the piconewton range acting on these objects. They are widely used in ''single-molecule'' experiments to study, for example, the mechanics of motor proteins and DNA-binding proteins,[1,2] but also to study the rheological properties of complex fluids.[3,4] A common optical tweezers setup consists of a near-infrared laser focused to a diffraction-limited spot in a light microscope using a high numerical-aperture objective. The interaction of the light with the refracting particle results in momentum transfer to the particle, which creates, under appropriate conditions, a three-dimensional potential well for the particle. Tied to momentum transfer to the particle is an equal and opposite change of momentum (i.e., primarily a change of the angular distribution) in the light beam which can be used to measure the exerted force or the particle displacement.[5–7] Using segmented photodiodes, displacement and force can be measured with nanometer and piconewton resolution. The technique has in principle a wide bandwidth, from hours (limited by the mechanical drift of the instrument) down to microseconds (limited by shot noise and electronics). In earlier applications it was noticed that the frequency response was unexpectedly attenuated above about 5 kHz.[8–10] We demonstrate here that this effect is due to the exponentially increasing transparency of silicon photodiodes when approaching the band gap energy in the near-infrared (~1100 nm).[11] This is a well-known fact, but not usually quantitatively elaborated on in manufacturers' catalogs.[11,12] As long as light is absorbed in the depletion layer of the photodiode, the response time is fast (nanoseconds). When, however, charge pairs are created outside this layer in the substrate, they will have to diffuse (microseconds) towards the depletion layer where they then contribute to the photocurrent, unless they have recombined before that. If the charge carrier diffusion time is smaller than the recombination time, the response time will be slowed down, in the opposite case the sensitivity will be decreased, without an effect on the response time. The depletion layer can be expanded by introducing an intrinsic (*I*) layer, or by applying a reverse bias voltage. There are specialized silicon photodiodes on the market (see later) that operate at a high reverse bias causing a complete depletion of the substrate, by which they maintain a fast response in the near infrared. Alternatively, standard InGaAs photodiodes have a band gap of ~1700 nm[13] and consequently do not suffer from this problem at 1064 nm.

A very accurate test for detection bandwidth is the observation of the Brownian motion of micron-sized particles in an optical trap. This Brownian motion has a well-known power spectral density of Lorentzian shape[14] for low frequencies. At higher frequencies inertial solvent effects modify the Lorentzian shape, again in a theoretically well-known manner.[15,16] We show that such solvent effects become measurable for beads with a size of about a micrometer in water above 10 kHz,[15,16] provided the proper detectors are used.

II. MATERIALS AND METHODS

We measured the Brownian motion of optically trapped microscopic beads in water and glycerol by backfocal-plane

[a]Electronic mail: erwinp@nat.vu.nl

interferometry,[6] using different detectors, laser wavelengths, and powers. We used silica beads with diameters of 500, 900, and 2200 nm (Bangs Laboratories, Fishers, IN) in water, and polystyrene beads of 502 nm diameter (Polysciences, Warrington, PA) in glycerol (water free, Fluka, Zwijndrecht, Netherlands). Beads were diluted typically to a concentration of 10^{-6} weight per volume and introduced into a sample chamber made of a cover slip and a microscope slide glued together with double-stick tape. Beads were trapped 10 μm above the cover slip water interface to limit frictional effects due to the interface to less then 5%.[17]

Two custom-built instruments were used for the experiments: one based on a Nd:YVO_4 laser (1064 nm, Compass 1064–4000 M, Coherent, Santa Clara, CA) and previously described in Ref. 6, and the other constructed similarly, based on a continuous-wave Ti:sapphire laser (Coherent Mira 900F with a triple-plate birefringent filter, pumped by a Coherent Verdi V10 frequency-doubled Nd:YVO_4 laser), tunable from 730 to 1000 nm. The detection optics of both setups consisted of a high-numerical-aperture condenser to collect the trapping laser light, with the backfocal plane of the condenser imaged onto a quadrant photodiode. For the present study we compared three different types of quadrant photodiode detectors: (i) a standard silicon *n*-type PN photodiode [10 mm diameter, SPOT 9-DMI, UDT, Hawthorne, CA (denoted Si–LB in the following)] operated with a reverse bias voltage of 15 V, (ii) an InGaAs PIN photodiode (G6849, Hamamatsu, Herrsching, Germany) (InGaAs) operated at a reverse bias voltage of 5 V, and (iii) a special purpose *p*-type, silicon, PN photodiode [YAG444-4A, Perkin Elmer, Vaudreuil, Canada (denoted Si–HB)]. This diode is especially designed for fast detection of 1064 nm light and was operated at a reverse bias voltage of 100 V.

The signals from the four quadrants of the diodes were amplified by low-noise, high-bandwidth preamplifiers (custom built) and the distribution of light on the diode was calculated by an analog normalizing differential amplifier (custom built).[7] The signals were then digitized with an analog-to-digital conversion board sampling at 195 kHz per channel (AD16 board on a ChicoPlus PC-card, Innovative Integration, Simi Valley, CA). This board is based on $\Sigma\Delta$ technology; hence, no external anti-alias filters were needed.

Time series of approximately 8 million points were recorded using custom-written LabView software (National Instruments, Austin, TX). Time series were Fourier-transformed using custom-written Microsoft Visual Basic programs using Component Works (National Instruments) fast Fourier transform routines. Spectra were smoothed by logarithmic binning. At the high-frequency end of the spectra, which we are mostly interested in here, several sources of experimental noise and error become important. Anti-alias filtering creates a systematic attenuation of the spectra, close to the Nyquist frequency. Electronic amplifier noise and light-level dependent shot noise on the other hand create a more or less flat noise bottom at high frequencies. Shot noise was minimized by using relatively high laser powers.

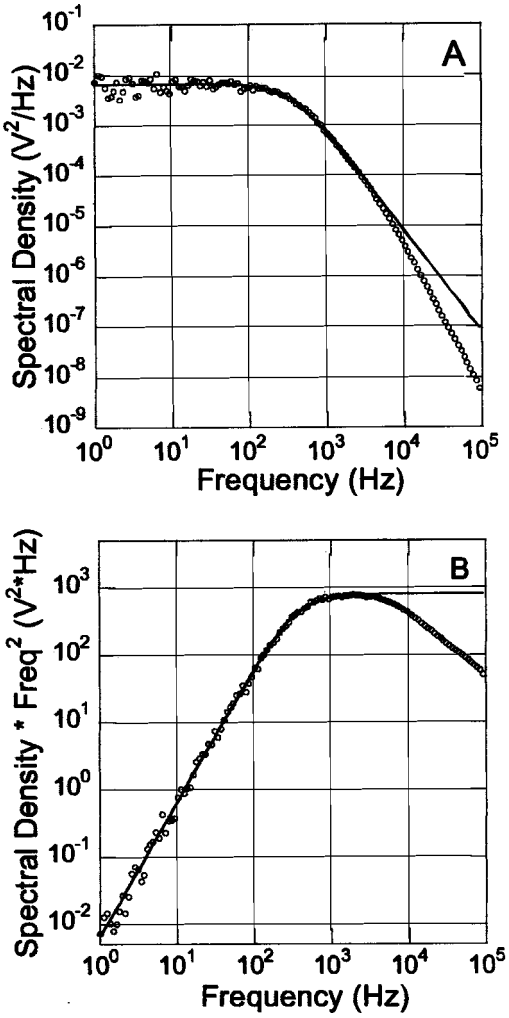

FIG. 1. (a) Power spectral density (circles) of the Brownian motion of a 900 nm diameter silica bead in water, trapped in the focus of a 30 mW, 1064 nm laser beam, detected with the standard silicon photodiode (Si–LB). The drawn line is a Lorentzian fitted to the data, with a corner frequency of 348 Hz. (b) Power spectral density and fit from (a) multiplied with the square of the frequency.

III. RESULTS AND DISCUSSION

A typical power spectral density of the Brownian motion of a 900 nm silica bead trapped with 1064 nm laser light and detected with the standard silicon diode (Si–LB) is shown in Fig. 1. The power spectrum is well fitted by a Lorentzian up to about 1 kHz. At higher frequencies the spectral density decreases substantially below the expected Lorentzian curve. In order to emphasize the high-frequency behavior, the power spectral density was multiplied with the square of the frequency [Fig. 1(b)]. Any deviation from a Lorentzian above the corner frequency shows up as a deviation from a horizontal line in this plot. To test whether the high-frequency attenuation is indeed caused by the wavelength-dependent decrease of response speed of standard silicon photodiodes we investigated the effect at different wavelengths. Power spectral densities of the Brownian motion of 900 nm beads trapped (and detected) at wavelengths between 750 and 1064 nm are shown in Fig. 2. It is evident that the attenuation increases strongly with wavelength. At wavelengths shorter than 850 nm the spectra become wavelength

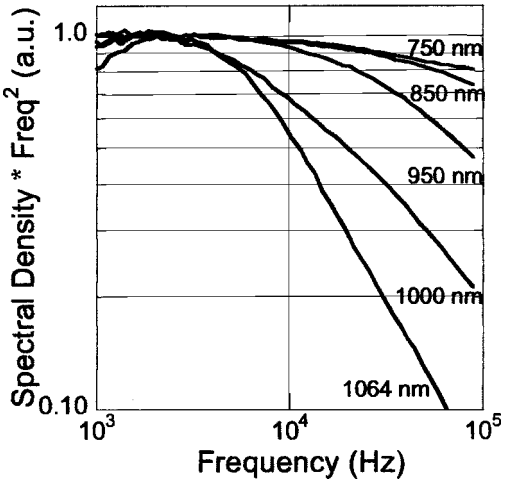

FIG. 2. Power spectral densities of the Brownian motion of 900 nm silica beads in water, trapped in the focus of a 1000, 950, 850, and 750 nm beam of a Ti:sapphire laser, detected with the standard silicon diode (Si–LB), multiplied with the square of the frequency. The power of the laser was adjusted such that the photocurrent generated in the photodiode was the same (0.5 mA) for these wavelengths. For comparison, the data at 1064 nm of Fig. 1 is added to the figure. The multiplied spectra were normalized to 1 in their maximum at about 1 kHz.

independent. A residual slight attenuation compared to the idealized Lorentzian curve shape remains even below 850 nm. This is caused by solvent inertia (see later). In Fig. 3 the response at 40 kHz, relative to the hydrodynamically corrected Lorentzian [Eq. (2)] is shown for many more wavelengths.

Rare-earth solid-state lasers with wavelengths around 1064 nm are frequently used for optical trapping, because of a good power:price ratio and particularly in biological systems where visible light causes photodamage.[18] Since changing the detection wavelength is not always an option, we searched the market for different types of detectors with better high-frequency response at 1064 nm. One alternative is

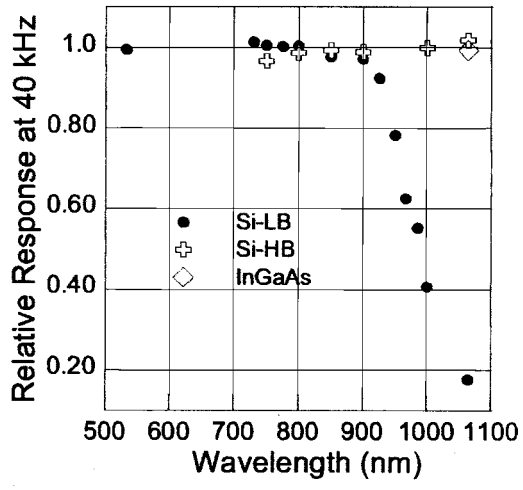

FIG. 3. The experimental response of the photodiodes at 40 kHz relative to the theoretical value [according to Eq. (2)] as a function of wavelength for the Brownian motion of a trapped 900 nm silica bead in water. Shown are data for the three photodiodes as indicated. The laser power was adjusted such that the photocurrent in the diodes at the different wavelengths was the same (0.5 mA). The data points at 1064 nm were measured on a different experimental setup.

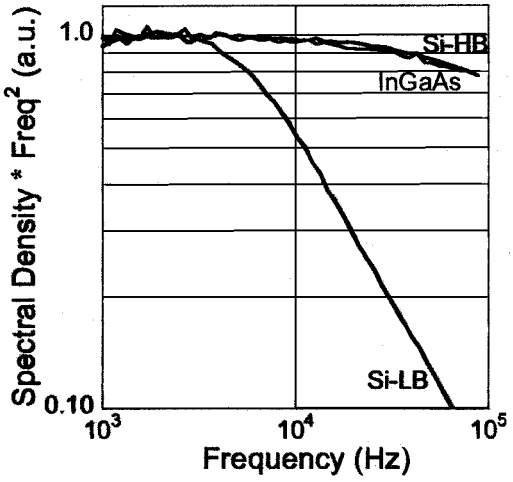

FIG. 4. Power spectral densities of the Brownian motion of 900 nm silica beads in water, trapped in the focus of a 1064 nm laser beam, multiplied with the square of the frequency. The three spectra were measured with different quadrant photodiodes as indicated (Si–LB:UDT SPOT 9-DMI, InGaAS: Hamamatsu G6849, and Si–HB: Perkin Elmer YAG444-4A).

an InGaAs PIN photodiode, with the response spectrum shifted to 900–1700 nm. A disadvantage of InGaAs quadrant detectors is that they are (to our knowledge) not available off-the-shelf with an active area larger than 2 mm diameter, consequently extra optics are needed to fit the image of the backfocal plane of the condenser on the diode. Figures 3 and 4 show that the InGaAs detector has a much better high-frequency response at 1064 nm than the silicon diode (Si–LB), similar to the silicon response at wavelengths below 850 nm.

The third detector tested was the specialized *p*-type silicon diode (Si–HB). This detector was operated at high reverse bias voltage (maximally 180 V, we applied 100 V), resulting in a fully depleted diode. In our setup this device had a much better high-frequency response at longer wavelengths than the standard silicon diode (Si–LB) (Figs. 3 and 4). Furthermore, the wavelength dependence of the response is much smaller than that of the standard Si diode.

The spectra measured with all three diodes under optimal conditions still deviate from a Lorentzian shape. To confirm that this remaining effect is not caused by the detectors, but rather by solvent inertia, we observed beads of different sizes in water and 502 nm beads in a more viscous solvent, glycerol (Fig. 5). The deviations from the Lorentzian curve shape between 10 and 100 kHz were strongly dependent on bead size and solvent. In glycerol, which has a 1000 times higher viscosity than water, the signal does not significantly deviate from a Lorentzian up to 100 kHz, confirming the absence of detector-caused attenuation. In water, spectra are clearly non-Lorentzian, increasingly so for larger beads. This is due to the neglect of solvent inertia in deriving the Lorentzian power spectrum.[14,16] Stokes' law, upon which the derivation is based, is only strictly valid for motion with constant velocity. In the case of a trapped Brownian bead the velocity is not constant. The appropriate solution of the Navier–Stokes equation, for the motion of a sphere in a viscous solvent is well known.[15,16] Due to solvent inertia a phase lag develops in the velocity field around the moving particle at a

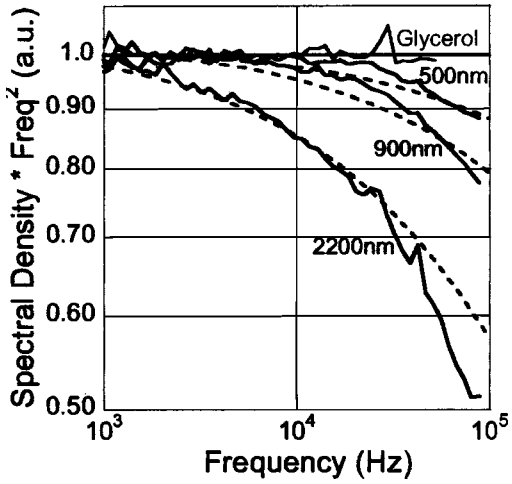

FIG. 5. Normalized power spectral densities multiplied with the square of the frequency of the Brownian motion of 502 nm polystyrene beads in glycerol, as well as of 500, 900, and 2200 nm silica beads in water. The glycerol data was cutoff at 50 kHz because at higher frequencies the data suffered from several spikes due to radio interferences. All the data were detected with the Si–HB detector and 1064 nm laser light. The dotted lines are equally treated calculated power spectra with hydrodynamic effects taken into account [Eq. (2)]. These spectra were calculated from the viscosity, bead size, and the corner frequency, without free fit parameters.

characteristic penetration depth δ, leading to additional friction force F_{fric}:[15]

$$F_{\text{fric}} = -6\pi\eta R\left(1+\frac{R}{\delta}\right)\dot{x} - \left(3\pi\rho R^2\delta + \frac{2}{3}\pi\rho R^3\right)\ddot{x},$$

$$\text{where} \quad \delta = \sqrt{\frac{\eta}{\pi\rho f}}. \tag{1}$$

η is the viscosity of the solvent, R is the radius of the sphere, ρ is the density of the solvent, x is the position of the sphere, and f is the frequency of the movement of the sphere. The characteristic length δ decreases with increasing frequency and increases with viscosity. When it becomes comparable to R, inertial effects are expected to become visible. The power spectral density of the Brownian motion of a trapped sphere can be expressed as[16]

$$P(f) = \frac{k_B T}{6\pi^3\eta R}\cdot\frac{[1+(f/f_\delta)^{1/2}]}{(f_c - f^{3/2}/f_\delta^{1/2})^2 + (f+f^{3/2}/f_\delta^{1/2})^2},$$

$$\text{where} \quad f_\delta = \frac{\eta}{\rho\pi R^2} \tag{2}$$

with the Boltzmann constant k_B and the absolute temperature T. In glycerol inertial effects are smaller than 0.01% of the restricted Brownian motion of the bead below 200 kHz, but in water they become clearly discernable for micrometer-sized beads at frequencies larger than 10 kHz, as can be seen in Fig. 5. There is qualitative agreement between the experimental and theoretical curves, although the shapes of the curves are not exactly identical. In order to fully explain the data, experimental noise, anti-alias filtering, and surface effects will have to be taken into account more quantitatively. Shot noise and electronic noise levels were always lower than the high-frequency ends of the measured spectra, as judged from their shape. The fact that the spectra decrease below the Lorentzian in a bead size dependent manner indicates that these noise sources as well as the anti-alias filtering do not have a major effect. Note that no free parameters were adjusted to construct the drawn lines. Input parameters are the bead size, viscosity, and the corner frequency obtained from a Lorentzian fit to the low-frequency part of the data.

In conclusion, we have shown improvements in the detectors that allow the measurement of power spectra of Brownian motion of trapped particles with high enough accuracy above 10 kHz such that hydrodynamic effects can be studied and compared to theoretical predictions. A more elaborate investigation of these hydrodynamic effects will be performed in the future.

ACKNOWLEDGMENTS

The authors thank Winfried Denk (Max-Planck-Institute for Medical Research, Heidelberg) for the idea that put us on the right track to solve this problem, Winfield Hill (Rowland Institute for Science) for help with the design and construction of the electronics, Ab Flipse and Maryam Atakhorrami for help with the experiments, Frederick Gittes (Washington State University) and Brandon Trombley for the first experiments years back, and Frederick MacKintosh, Kirstine Berg-Sørensen, Henryk Flyvbjerg, and Lene Oddershedde for helpful discussions. This research was supported by the Foundation for Fundamental Research on Matter (FOM). E.P. is supported by a PULS-fellowship from the Research Council for Earth and Life Sciences (ALW) with financial aid from the Dutch Organization for Scientific Research (NWO).

[1] C. Bustamante, J. C. Macosko, and G. J. L. Wuite, Nat. Rev. Mol. Cell Biol. **1**, 130 (2000).
[2] F. Gittes and C. F. Schmidt, Curr. Opin. Solid State Mater. Sci. **1**, 412 (1996).
[3] F. C. MacKintosh and C. F. Schmidt, Curr. Opin. Colloid Interface Sci. **4**, 300 (1999).
[4] L. A. Hough and H. D. Ou-Yang, Phys. Rev. E **65**, 021906 (2002).
[5] S. B. Smith, Y. J. Cui, and C. Bustamante, Science **271**, 795 (1996).
[6] F. Gittes and C. F. Schmidt, Opt. Lett. **23**, 7 (1998).
[7] M. W. Allersma, F. Gittes, M. J. deCastro, R. J. Stewart, and C. F. Schmidt, Biophys. J. **74**, 1074 (1998).
[8] F. Gittes, B. Schnurr, P. D. Olmsted, F. C. MacKintosh, and C. F. Schmidt, Phys. Rev. Lett. **79**, 3286 (1997).
[9] C. Veigel, M. L. Bartoo, D. C. S. White, J. C. Sparrow, and J. E. Molloy, Biophys. J. **75**, 1424 (1998).
[10] K. Berg-Sorensen, L. Oddershede, E. L. Florin, and H. Flyvbjerg, J. Appl. Phys. **93**, 3167 (2003).
[11] Hamamatsu, *Si PHOTODIODES* [Hamamatsu Photonics KK, Hamamatsu City, Japan (www.hamamatsu.com), 2002].
[12] UDT, *Photodiode Characteristics* [UDT Sensors Inc., Hawthorne, CA (www.udt.com), 2002].
[13] Hamamatsu, *InGaAs PIN PHOTODIODE* [Hamamatsu Photonics KK, Hamamatsu City, Japan (www.hamamtsu.com), 2001].
[14] F. Gittes and C. F. Schmidt, Methods Cell Biol. **55**, 129 (1998).
[15] L. D. Landau and E. M. Lifshitz, *Fluid Mechanics*, 2nd ed. (Pergamon, Oxford, 1987).
[16] K. Berg-Sorensen and H. Flyvbjerg (unpublished).
[17] J. Happel and H. Brenner, *Low Reynolds Number Hydrodynamics* (Kluwer Acedemic, Dordrecht, 1991).
[18] K. C. Neuman, E. H. Chadd, G. F. Liou, K. Bergman, and S. M. Block, Biophys. J. **77**, 2856 (1999).